3D Visualization of Objects in Heavy Scattering Media by Using Wavelet Peplography

doi: https://doi.org/10.1109/ACCESS.2022.3231742

IEEE Access
Multidisciplinary | Rapid Review | Open Access Journal

Received 29 November 2022, accepted 19 December 2022, date of publication 22 December 2022,
date of current version 29 December 2022.

Digital Object Identifier 10.1109/ACCESS.2022.3231742

RESEARCH ARTICLE

3D Visualization of Objects in Heavy Scattering Media by Using Wavelet Peplography

JAEHOON LEE[1], MYUNGJIN CHO[2], AND MIN-CHUL LEE[1]

[1]Department of Computer Science and Networks, Kyushu Institute of Technology, Iizuka, Fukuoka 820-8502, Japan
[2]Research Center for Hyper-Connected Convergence Technology, School of ICT, Robotics, and Mechanical Engineering, IITC, Hankyong National University, Anseong, Kyonggi 17579, South Korea

Corresponding author: Min-Chul Lee (lee@csn.kyutech.ac.jp)

This work was supported by the Kyushu Institute of Technology, On-Campus Support Program 2022.

ABSTRACT In this paper, we propose three-dimensional(3D) visualization of objects in heavy scattering media by using peplography and wavelet transform. Conventional haze removal techniques can remove the light haze in the image by using various image processing algorithms or machine learning techniques. However, they may not provide a clear image under heavy scattering media. On the other hand, peplography can visualize the object by detecting ballistic object photons from heavy scattering media. Then, 3D image can be generated by integral imaging. However, it may not visualize 3D object information accurately because of the noise photons from scattering media. Therefore, the image quality for 3D object visualization may be degraded. To solve this problem, we use the discrete wavelet transform in peplography. It can detect the object photon signals from the scattering media and enhance 3D image contrast ratio by using a specific coefficient threshold technique. To prove our method, we carry out optical experiments and compare results with the conventional haze removal method and peplography by using various image quality metrics such as correlation, structural similarity, and peak signal-to-noise ratio.

INDEX TERMS 3D visualization, wavelet transform, scatter media removal, photon-starved conditions, photon counting imaging, statistical optics.

I. INTRODUCTION

Recently, visualization under the high-density scattering media is a consequential challenge in many industry fields. Especially, the autonomous vehicle utilizes LiDAR [1], [2] and a camera to recognize the object in front of the car. However, LiDAR is difficult to visualize the object under inclement weather conditions. Therefore, it can cause a critical recognition error for the autonomous vehicle. On the other hand, the camera can visualize the object with proper shape and color. Thus, image processing through the camera is significant for accurate object recognition under scattering media conditions. Many researchers have proposed single image dehazing technique [3], [4], [5], [6], [7] and utilized machine learning techniques such as convolution neural network and generative adversarial network [8], [9], [10] to recover the image under these conditions. Their methods can recover the scene accurately in the light scattering media or the specific haze image dataset. However, their methods need much optical equipment, such as a polarizer, and composing the complicated scattering media filtering optical systems is challenging. Therefore, utilizing the systems in various industrial fields is difficult. Moreover, it is difficult to visualize the object under heavy scattering media conditions. To visualize the scene under these conditions using a conventional camera, peplography [11] has been proposed. It can visualize the object under the scattering media by photon counting integral imaging [21], [22], [23], [24], [25], [26], [27], [28] and statistical estimation. Peplography can estimate and remove the scattering media components from the scene by central limit theorem and maximum likelihood estimation. Then, using photon counting imaging [12], [13], [14], [15], it can detect ballistic photons from the scene. Therefore, it can visualize the

The associate editor coordinating the review of this manuscript and approving it for publication was Wen Chen.

object well even under heavy scattering media. Moreover, it can utilize integral imaging [16], [17], [18], [19], [20] to enhance the image quality and generate the 3D information of the scene.

Integral imaging is the one of passive 3D image acquisition and reconstruction technique that does not require a coherent light source and special viewing devices. It uses the lens array to obtain the different perspective information from the 3D scene and can reconstruct the 3D image by volumetric computational reconstruction (VCR) [18]. VCR uses elemental images which have different perspectives of the 3D scene and reconstructs 3D image on the reconstruction plane by overlapping the elemental images through the virtual pinhole array.

Peplography uses the photon counting image that contains ballistic object photons from the heavy scattering media as the elemental image and then it can reconstruct the 3D image using VCR. However, it may not provide sufficient 3D object information and image quality due to the lack of ballistic photons from heavy scattering media, and the measured ballistic photon has intensity fluctuation. Moreover, since VCR uses the averaging calculation, it may reduce the photon pixel intensity. To solve these problems, in this paper, we propose wavelet peplography which can enhance the visual quality of the 3D image and reduce the noise photons from the scattering media by 2D discrete wavelet transform [29], [30], [31], [32], [33], [34]. Our proposed method analyzes the information of ballistic photons through the multi-level decomposition of the discrete wavelet transform to recognize the noise photons in the scene. Then, it utilizes the novel threshold technique to reduce the noise photons without object information loss. Since noise photons are reduced in the scene, it can enhance the image contrast ratio and visual quality. Moreover, our proposed method can reduce the object photon intensity fluctuation through the noise removal technique and integral imaging computational reconstruction technique. Finally, it can generate a more accurate 3D image compared with conventional dehazing techniques and peplography even under low luminance scattering media conditions.

This paper is organized as follows. We present the conventional scattering media removal technique in Section 2. Then, we depict our proposed method in Section 3. To prove our proposed method, we compare it with conventional methods through various optical experiments under different scattering media conditions. In addition, we calculate the various image metrics to prove the feasibility of our proposed method in Section 4. Finally, we present the conclusion in Section 5.

II. CONVENTIONAL SCATTERING MEDIA REMOVAL TECHNIQUES

3D visualization of objects under scattering media becomes a significant problem in many research fields. Especially, the autonomous vehicle requires an optimum decision to avoid the accident under scattering media road conditions. However, if the camera may not visualize the scene sufficiently for the optimum decision, it may cause a critical accident. To remove the scattering media effectively, researchers have been proposed a lot of methods such as polarization imaging [3], gamma correction, dark channel prior [4], single-pixel imaging [7], and machine learning which uses deep convolution neural network [10] through the numerous scattering media image data and so on. Fig. 1 shows the result images by multi-scale boosted dehazing network with dense feature fusion (MSBDN-DFF).

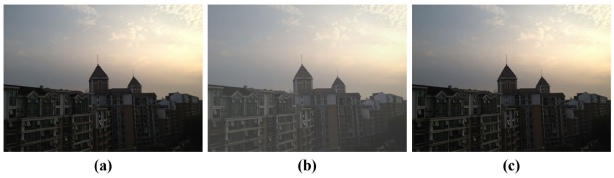

FIGURE 1. Scattering media removal by using deep convolution neural network. (a) Reference image, (b) hazy image, and (c) processed image.

Conventional dehazing methods may recover the image accurately under light scattering media conditions. However, some of them may not provide accurate object information under heavy scattering media conditions. Therefore, it is still a challenge to recover the image under these conditions. On the other hand, peplography may remove the heavy scattering media from the image effectively [11]. The origin of word "peplography" comes from greek $\pi\acute{\epsilon}\pi\lambda o$ (peplo; "veiled") and $\gamma\rho\alpha\varphi\acute{\eta}\zeta$ (grafis; "writing"). In addition, images captured under heavy scattering media are called peplogram. Peplography can estimate and remove the scattering media through the statistical method. After that, it can detect the ballistic photons from the image for visualization by photon counting imaging. Finally, it can enhance the visual quality of the image and obtain the 3D information by VCR. Fig. 2 shows the concept of peplography.

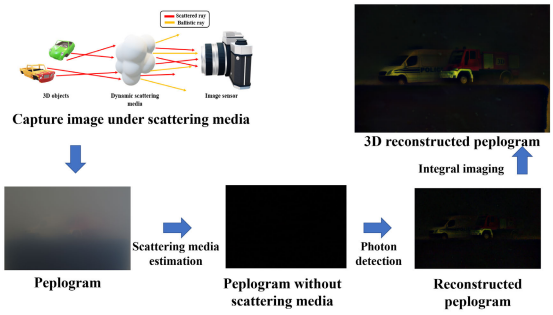

FIGURE 2. Concept of peplography.

To estimate the scattering media from the scene, maximum likelihood estimation (MLE) can be used. Since scattering media are composed of various local scattering media with size of w_x and w_y respectively, they are assumed to be Gaussian distribution with mean μ_{ij} and a variance σ_{ij}^2 by central limit theorem, where i and j represent the index of each scattering medium in x and y directions, respectively. Finally, the local scattering medium can be defined as follows [11]:

$$X_{ij}(m, n) = I_p(i + m - 1, j + n - 1),$$

$$
\begin{aligned}
&i = 1, 2, \ldots, N_x - w_x + 1 \\
&j = 1, 2, \ldots, N_y - w_y + 1, \\
&\text{for} \\
&m = 1, 2, \ldots, w_x \\
&n = 1, 2, \ldots, w_y
\end{aligned} \tag{1}
$$

where I_p represents the pixel intensity of the peplogram which is the image from the scattering media, X_{ij} is the local scattering medium, and N_x, N_y refer the number of pixels of each peplogram, respectively. To estimate the scattering media, Gaussian distribution and MLE are used as follows [11]:

$$
\begin{aligned}
&L(X_{ij}(m,n)|\mu_{ij}, \sigma_{ij}^2) \\
&= \prod_{m=1}^{w_x} \prod_{n=1}^{w_y} \frac{1}{\sqrt{2\pi\sigma^2}} \exp\left[-\frac{\{x_{ij}(m,n) - \mu_{ij}\}^2}{2\sigma_{ij}^2} \right] \\
&= \frac{1}{\sqrt{2\pi\sigma^2}} \exp\left[-\sum_{m=1}^{w_x} \sum_{n=1}^{w_y} \frac{\{x_{ij}(m,n) - \mu_{ij}\}^2}{2\sigma_{ij}^2} \right].
\end{aligned} \tag{2}
$$

For calculation convenience, we take the logarithm of (2). Then, the following equation can be obtained [11].

$$
\begin{aligned}
&l\left\{x_{ij}(m,n)|\mu_{ij}, \sigma_{ij}^2\right\} \\
&= \ln\left(\frac{1}{\sqrt{2\pi\sigma^2}}\right) - \sum_{m=1}^{w_x} \sum_{n=1}^{w_y} \frac{\{x_{ij}(m,n) - \mu_{ij}\}^2}{2\sigma_{ij}^2}.
\end{aligned} \tag{3}
$$

Finally, the scattering media can be estimated by MLE as follows [11]:

$$
\begin{aligned}
\hat{\mu}_{ij} &= \arg\max_{\mu_{ij}} l\left\{x_{ij}(m,n)|\mu_{ij}, {\sigma^2}_{ij}\right\} \\
&= \frac{1}{w_x w_y} \sum_{m=1}^{w_x} \sum_{n=1}^{w_y} x_{ij}(m,n).
\end{aligned} \tag{4}
$$

From (4), it is noticed that the estimated scattering media is the mean of the local scattering medium. Finally, the estimated scattering media can be removed from the peplogram by the following [11]:

$$
\tilde{I}_p(i,j) = I_p(i,j) - \hat{\mu}_{ij} \tag{5}
$$

where $I_p(i,j)$ represents the peplogram, $\hat{\mu}_{ij}$ is the estimated scattering media, and $\tilde{I}_p(i,j)$ is the peplogram without scattering media. Now, the sparse ballistic object photons can be detected from the peplogram without scattering media by the computational photon counting imaging, which is modelled by the Poisson random process by (6) and its concept is illustrated in Fig. 3 [21].

$$
C_{ij}|\tilde{I}_p(i,j) \sim Poisson[N_p \times \tilde{I}_p(i,j)] \tag{6}
$$

where N_p is the number of ballistic photons from the peplogram without scattering media and C_{ij} is the reconstructed peplogram.

However, photon counting imaging may detect the undesired photons from scattering media and they may disturb the image quality of 3D visualization. Moreover, if the 3D object is located under the dark smoke situation, it is difficult to recognize the object accurately. To enhance the image quality and acquire accurate 3D information, integral imaging can be used. Fig. 4 illustrates the concept of integral imaging. It can record 3D information from the scene and display 3D image by lens array.

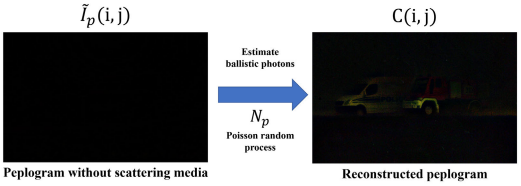

FIGURE 3. Concept of computational photon counting model.

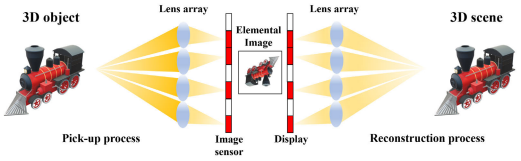

FIGURE 4. Integral imaging.

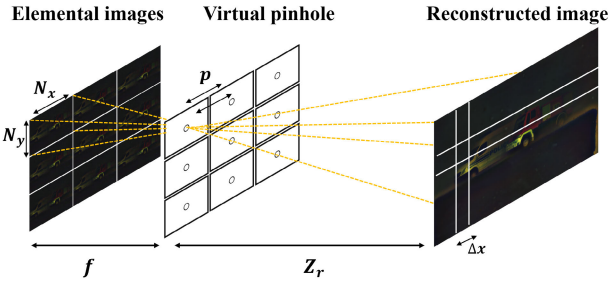

FIGURE 5. Volumetric computational reconstruction.

To reconstruct a 3D image by computational method, volumetric computational reconstruction (VCR) can be used as shown in Fig. 5. VCR is one of the computational integral imaging reconstruction technique. It can generate 3D information by overlapping multiple 2D images with different perspectives on the reconstruction plane through the virtual pinhole array, where these 2D images are referred to as elemental images. In addition, it may enhance the image quality of 3D images due to averaging calculation. VCR process can be defined as follows [16] and [21].

$$
\Delta x = \frac{N_x p f}{c_x z_r}, \quad \Delta y = \frac{N_y p f}{c_y z_r} \tag{7}
$$

$$
\begin{aligned}
&R_c(x, y, z_r) \\
&= \frac{1}{N_p O(x, y, z_r)} \sum_{k=0}^{K-1} \sum_{l=0}^{L-1} C_{(k,l)}(x + k\Delta x, y + l\Delta y)
\end{aligned} \tag{8}
$$

where Δx, Δy represent the shifting pixel value of each elemental image for 3D reconstruction, N_x, N_y are the number of the pixels of each elemental image, p is the distance between virtual pinholes, f is the focal length, z_r is the reconstruction

depth, c_x, c_y are the sensor size, $C_{(k,l)}$ represents the reconstructed peplogram, and $R_c(x, z_r)$ is the reconstructed 3D peplogram, respectively. 3D reconstructed peplogram may have better image quality than the single 2D reconstructed peplogram even under heavy scattering media conditions. However, since the 2D reconstructed peplogram still contains the scattering media photons (i.e., noise photons), it may degrade the pixel intensity of 3D reconstructed peplogram by average calculation. To overcome these problems, in this paper, we propose wavelet peplography which can reduce scattering media photons and enhance the contrast ratio of 2D reconstructed peplogram by the discrete wavelet transform filtering technique.

III. PROPOSED METHOD

A. WAVELET TRANSFORM

2D Fourier transform is generally used for the frequency analysis of 2D signal. It decomposes 2D signal with infinite sine waves in each axis, respectively. Therefore, It is useful to analyze the main frequency components of 2D signal. However, 2D Fourier transform may not provide the signal information in time domain. In addition, inverse Fourier transform may compose a different signal compared with the input signal. To overcome these problems, wavelet transform [29], [30], [31], [32], [33] can be used. Wavelet transform utilizes the wavelet function to analyze the signal in both time and frequency domains. It shifts the wavelet function by using manually defined shifting and scaling values. Therefore, it may provide higher frequency resolution compared with the Fourier transform. However, it has the high calculation cost and takes time to analyze 2D signal. Thus, most image processing researches use 2D discrete wavelet transform that already defines the shifting and scaling values uniformly. 2D discrete wavelet transform can be defined as follows [29], [30], [31], and [32]:

$$\phi_{s,u,v}(x, y) = 2^{\frac{s}{2}}\phi(2^s x - u, 2^s y - v) \tag{9}$$

$$\psi^d_{s,u,v}(x, y) = 2^{\frac{s}{2}}\psi^d(2^s x - u, 2^s y - v)(d = H, V, D) \tag{10}$$

where s is the decomposition level, d is the decomposition direction, and u, v represents the translation of each direction. 2D discrete wavelet transform uniformly changes the scaling and shifting indexes to detect various frequency components in the scene. $\phi_{s,u,v}(x, y)$ is a scaling function which is used as the low-pass filter in wavelet transform and generates the approximation term. $\psi^d_{s,u,v}(x, y)$ is the wavelet function which can analyze the frequency components with three kinds of detail coefficients such as horizontal(H), vertical(V), and diagonal(D), respectively. Moreover, approximation term can be reused as the image and generate the other detail coefficients. Therefore, it can represent the various frequency components with multiple decomposition levels. It is called multi-level decomposition analysis. It can be depicted in Fig. 6.

Approximation term represents low-frequency components in the image and three coefficients represent the high-frequency components in the specific level of multi-level decomposition. Through the decomposition, it can remove the specific frequency noise, and it can also emphasize the meaningful information in the scene. Our proposed method uses 2D discrete wavelet transform and specific coefficient threshold technique to remain meaningful photons according to the characteristics of 2D reconstructed peplogram. Therefore, it can enhance the image quality of 2D reconstructed peplogram under heavy scattering media conditions.

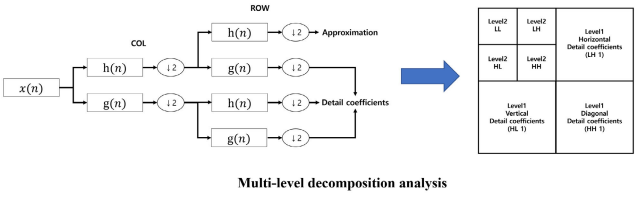

FIGURE 6. Multi-level decomposition analysis.

B. WAVELET PEPLOGRAPHY

The conventional peplography uses only photon counting imaging to detect meaningful photons from the peplogram without scattering media. Since photons are detected with discrete shapes through the Poisson random process and this process can detect not only the object photons but also the scattering media photons, the visual quality of 2D reconstructed peplogram may be reduced. Therefore, due to the lack of object photons, sufficient information may not be provided under dark scattering media conditions. Our proposed method utilizes 2D discrete wavelet transform to maintain the meaningful photons and reduce the scattering media photons through the multi-level decomposition using the adaptive threshold value. Fig. 7 shows the concept of our proposed method.

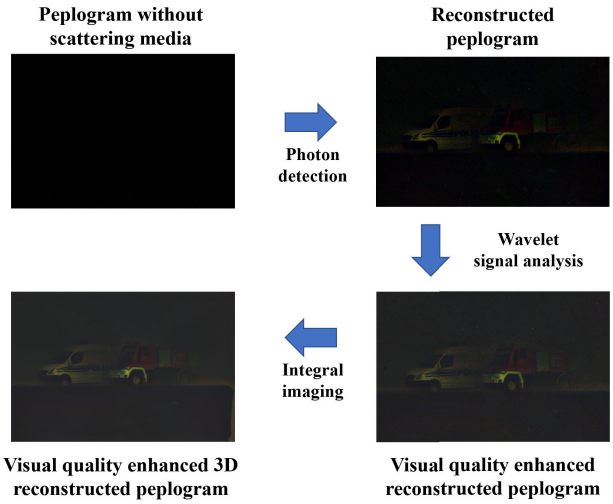

FIGURE 7. Concept of the proposed method.

Since photon counting image intensity is referred to as the possibility of the photons occurrence, object photon

represents higher pixel intensity than noise photons. Moreover, the coefficient of object photons shows the specific characteristic when decomposed into various decomposition levels. Therefore, it can distinguish the object photons and noise photons in the scene. (11) and (12) represent the multi-level decomposition of 2D reconstructed peplogram [29], [30], [31], [32].

$$A_\phi(s_0, u, v) = \frac{1}{\sqrt{UV}} \Sigma_{x=0}^{U-1} \Sigma_{y=0}^{V-1} C(x, y) \phi_{s_0,u,v}(x, y) \quad (11)$$

$$E_\psi^d(s, u, v) = \frac{1}{\sqrt{UV}} \Sigma_{x=0}^{U-1} \Sigma_{y=0}^{V-1} C(x, y) \psi_{s,u,v}^d(x, y) \quad (12)$$

$A_\phi(s_0, u, v)$ is approximation term, and $E_\psi^d(s, u, v)$ is the detail coefficients in each decomposition level and direction, respectively. In the first level decomposition, wavelet transform uses the first wavelet function that is appropriate to detect high-frequency components in the scene. Since object photons have high intensity values in the image, they can be detected in the first decomposition. Fig. 8 shows the coefficient values of 2D reconstructed peplogram according to the various decomposition levels.

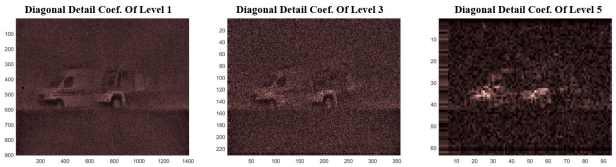

FIGURE 8. Coefficients of 2D reconstructed peplogram in (a) decomposition level 1, (b) decomposition level 3, and (c) decomposition level 5.

As the decomposition level increases, the approximation term is compressed according to the scaling function. Since the object photon has a relatively higher photon density compared with the scattering media photon in the scene, it becomes the low-frequency component as it merges with adjacent object pixels through the scaling function. On the other hand, the scattering media photons show a small peak coefficient value as the decomposition level increases. To classify and reduce the scattering media photon components, our proposed method uses the multi-level decomposition as following equations.

$$W_t = \frac{\hat{N}_p}{N_p} \quad (13)$$

$$P_s = \begin{cases} W_t / \arg\max E_\psi^d(s, u, v)\ (0 < W_t < 1) & \text{if } s = 1 \\ \dfrac{P_1}{2^{s-1}} & \text{if } s \geq 2 \end{cases} \quad (14)$$

$$T_s = \arg\max(E_\psi^d(s, u, v)) * P_s \quad (15)$$

W_t is the photon ratio of the image. Our proposed method uses the number of photons N_p as much as the number of image pixels. $\hat{N}_p$ is the number of measured photons in the image. $E_\psi^d(s, u, v)$ represents the coefficient value. P_s is the threshold ratio and T_s is the coefficient threshold value in each decomposition level. The coefficient threshold value can be adjusted according to measured photons in the scene. If the scene contains a lot of objects and scattering media, many measured photons can be extracted. On the other hand, the number of measured photons may be decreased when the image has a few objects and scattering media in the scene. In addition, the light condition also influences the number of measured photons. If the scene contains a lot of measured photons, both the noise and meaningful photons increase simultaneously. Therefore, the high photon ratio is needed. In contrast, if measured photons are insufficient, the low photon ratio is adequate to visualize the scene. Thus, our proposed method can remove the scattering media effectively under various light conditions. Then, the enhanced reconstructed peplogram can be generated by using inverse wavelet transform as follows:

$$E_\psi^d(s, u, v) = \begin{cases} 0 & E_\psi^d(s, u, v) < T_s \\ E_\psi^d(s, u, v) & E_\psi^d(s, u, v) \geq T_s \end{cases} \quad (16)$$

$$Q(x, y) = \frac{1}{\sqrt{UV}} \Sigma_{u=0}^{U-1} \Sigma_{v=0}^{V-1} A_\phi(s_0, u, v) \phi_{s_0,u,v}(x, y) + \frac{1}{\sqrt{UV}} \Sigma_{u=0}^{U-1} \Sigma_{v=0}^{V-1} E_\psi^d(s, u, v) \psi_{s,u,v}^d(x, y) \quad (17)$$

$E_\psi^d(s, u, v)$ represents the filtered coefficients in each decomposition level. Scattering media coefficients are removed in each decomposition level using our specific threshold technique. Then, our proposed method generates the enhanced reconstructed peplograms through inverse wavelet transform using the same scaling and wavelet functions used for decomposition. Finally, visual quality enhanced peplogram $Q(x, y)$ can be generated. Fig. 9 shows the coefficient difference between the conventional and proposed method.

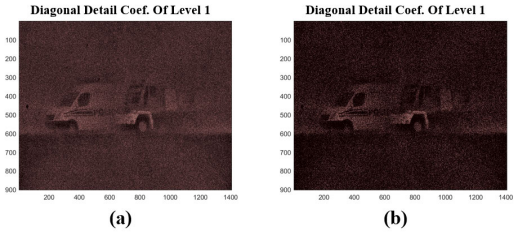

FIGURE 9. Coefficient difference. (a) conventional peplography and (b) proposed method.

The reconstructed peplogram coefficient still contains the haze components. However, our proposed method reduces the scattering media coefficients without object photon coefficient loss to enhance the visual quality of the reconstructed peplogram. Even if our proposed method occurs coefficient loss, it can recover the object information by utilizing the other level decomposition coefficients. Since scattering media photons are removed from the scene, the image contrast ratio and visualization can be enhanced. To generate the

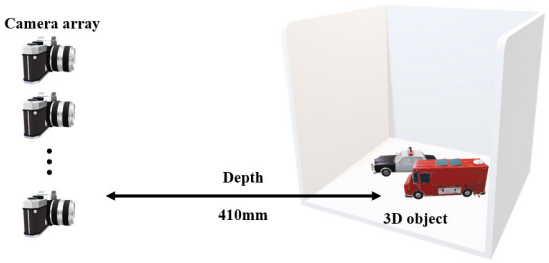

FIGURE 10. Optical experiment setup.

3D information of the object and enhance the visual quality, integral imaging can be used as follows:

$$R_w(x, y, z_r) = \frac{1}{N_p O_w(x, y, z_r)} \sum_{k=0}^{K-1} \sum_{l=0}^{L-1} Q_{kl}(x + k\Delta x, y + l\Delta y) \quad (18)$$

where Q_{kl} represents visual quality enhanced reconstructed peplogram and $R_w(x, y, z_r)$ is 3D reconstructed peplogram. As a result, our proposed method can visualize 3D object more accurately compared to conventional peplography even under various scattering media situations.

Since conventional peplography may detect photons from the scattering media, it may not effectively generate 3D object information. Moreover, the image quality may be degraded due to the photon intensity fluctuations through the Poisson random process. Therefore, it may not provide accurate 3D information under the dark scattering media. In contrast, our proposed method can reduce the noise photons by using 2D wavelet transform multi-level decomposition. We can utilize an adequate threshold value in each decomposition level coefficient and distinguish the object photons while minimizing information loss according to the scattering media environment.

Finally, our proposed method can effectively visualize the 3D object under various scattering media conditions. To prove our proposed method, we implemented two optical experiments under heavy scattering media with normal light and dark situations. To represent the performance of our proposed method, we evaluated the single 2D reconstructed peplogram and 3D reconstructed peplogram, respectively. We used various image quality metrics such as correlation, peak signal-to-noise ratio (PSNR), and structural similarity (SSIM).

IV. OPTICAL EXPERIMENTS AND SETUP

To capture the elemental images (i.e., peplograms) under the scattering media situation, we used 9(H) × 9(V) camera array. The camera focal length is 50mm and the pitch between cameras is 2mm. Each elemental image resolution is 3008(H) × 2000(V). Fig. 10 shows our optical experiment setup.

We gradually added the milk to the water tank until the scene seemed to be the heavy scattering media condition. To assume the various light conditions under the scattering media, we captured elemental images under different light conditions. To reduce the noise photons in the photon counting image by using discrete wavelet transform, Daubechies wavelet function [30] was used.

A. SCATTERING MEDIA UNDER NORMAL LIGHT CONDITION

Since we assumed the heavy scattering media situation under normal light condition, we irradiated sufficient light into the turbid water tank. Therefore, it is hard to recognize 3D object in the scene under the scattering media. Fig. 11 shows the single 2D peplogram under normal light condition.

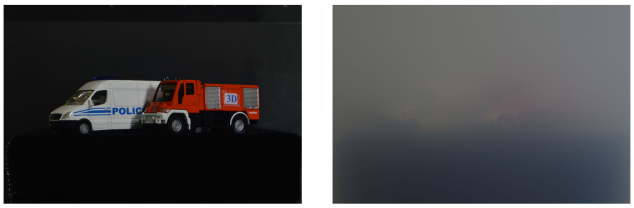

FIGURE 11. Scattering media under normal light condition. (a) reference image and (b) 2D peplogram.

We implemented three different scattering media removal methods to visualize the object in the scene. First, we utilized a machine learning technique (MSBDN-DFF) that can remove the scattering media. To train the network, we used the RESIDE dataset [35] that contains hazy and clean image pairs of indoor and outdoor scenes. To enhance the network accuracy, mean square error (MSE) was used as a loss function, and the ADAM was utilized as an optimizer. The number of epochs was 100. Other methods are conventional peplography and proposed wavelet peplography which measure 6,016,000 photons N_p in each elemental image. Fig. 12 shows the single 2D reconstructed peplograms.

FIGURE 12. 2D reconstructed peplogram by (a) MSBDN-DFF, (b) conventional peplography, and (c) proposed wavelet peplography.

MSBDN-DFF may remove scattering media accurately under light scattering media situation. However, it cannot visualize the object under heavy scattering media condition as shown in Fig. 12 (a). Conventional peplography can extract the object photons from the peplogram as shown in Fig. 12 (b). However, it contains scattering media photons that may reduce the image quality. On the other hand, our proposed method can recognize noise components using 2D

discrete wavelet transform and filter the noise coefficients according to the photon ratio W_t as shown in Fig. 12 (c). Then, it can visualize the object more accurately and enhance the image contrast ratio. To acquire 3D information through VCR, we used 2D reconstructed peplograms by conventional peplography and wavelet peplography as elemental images. Fig. 13 shows 3D reconstructed peplograms.

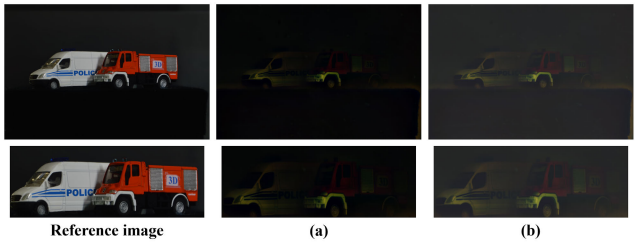

FIGURE 13. 3D reconstructed peplogram by (a) conventional peplography and (b) proposed wavelet peplography.

The computational reconstruction of integral imaging (i.e., VCR) may reduce the noise through the averaging calculation. Therefore, both results may provide object information more accurately compared with single 2D reconstructed peplogram as shown in Fig. 13. However, the conventional peplography may degrade the pixel value due to the discrete photon intensity fluctuations. However, our proposed method can maintain the object photon intensity smoothly and reduce the noise photons by using wavelet transform. Therefore, it can be effective to visualize 3D object under heavy scattering media condition by using VCR. To evaluate the image quality via various reconstruction depths, we calculated several image quality metrics, as shown in Fig. 14.

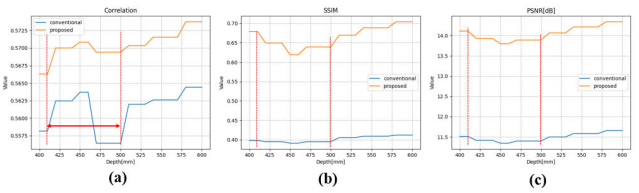

FIGURE 14. Image quality metrics via various reconstruction depths. (a) correlation, (b) structural similarity, and (c) peak signal to noise ratio.

Our proposed method has better image quality metrics than the conventional peplography overall, as shown in Fig. 14. Especially, the correlation result of conventional peplography as shown in Fig. 14 (a) rapidly decreases from 410mm to 500mm where the two objects are placed. Table 1 shows the detailed image metrics value in specific depths between 430mm and 470mm.

Since our proposed method maintains the value of the metrics even at increasing reconstruction depth, it proves that our proposed method can visualize 3D object under the heavy scattering media situation more accurately compared to the conventional method. Moreover, to demonstrate the performance of our proposed method under photon-starved conditions, we adjusted the amount of light irradiation and used the same heavy scattering media condition.

TABLE 1. Image metric differences in specific depths.

		430mm	450mm	470mm
Conventional	Correlation	0.5624	0.5637	0.5564
	SSIM	0.3951	0.3911	0.3950
	PSNR	11.4176	11.3459	11.3992
Proposed	Correlation	**0.5700**	**0.5708**	**0.5694**
	SSIM	**0.6493**	**0.6191**	**0.6391**
	PSNR	**13.9322**	**13.7987**	**13.8896**

B. SCATTERING MEDIA UNDER THE DARK CONDITION

Visualizing the object under the photon-starved heavy scattering media is also challenge. In this experiment, we tried to extract the photons and visualize 3D object using our proposed method. We irradiated a few amounts of light into the turbid water tank to compose the low luminance scattering media situation. Fig. 15 shows the reference image and dark peplogram.

FIGURE 15. Scattering media under the dark condition. (a) reference image and (b) peplogram.

When the light source is insufficient, it is hard to extract meaningful photons from the scene. Thus, we measured 6,016,000 photons, N_p from the scene. Since measured photons $\widehat{N}_p$ may be decreased compared with the previous optical experiment, the low photon weight value W_t was used to maintain the meaningful photons in the scene. Fig. 16 shows 2D reconstructed peplograms under the dark scattering media situation.

The MSBDN-DFF as shown in Fig. 16 (a) may not visualize the object under dark condition. The conventional peplography as shown in Fig. 16 (b) removed the scattering media better than MSBDN-DFF. However, the photons from scattering media may veil the object under the photon-starved heavy scattering media situation. On the other hand, our proposed method as shown in Fig. 16 (c) segmented the meaningful photons. It can remove the noise and emphasize the object photons through the adaptive threshold value in various wavelet decomposition levels. Finally, we used VCR to generate 3D object depth information under the dark situation. Since MSBDN may not visualize objects accurately, we only compare the conventional peplography and the proposed method results. Fig. 17 shows 3D reconstructed peplograms, respectively.

Since the conventional peplography may decrease the photon intensity of 3D reconstructed peplogram by averaging calculation of the reconstruction process as shown in Fig. 17 (a), it is difficult to visualize 3D object. In contrast, our

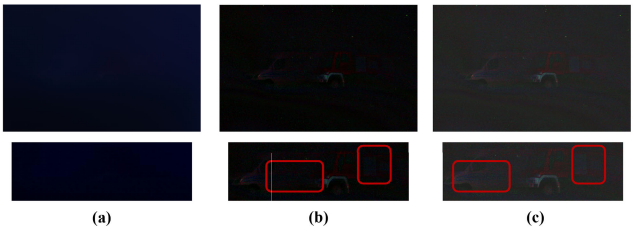

FIGURE 16. Reconstructed peplograms by (a) MSBDN-DFF, (b) conventional peplography, and (c) proposed wavelet peplography.

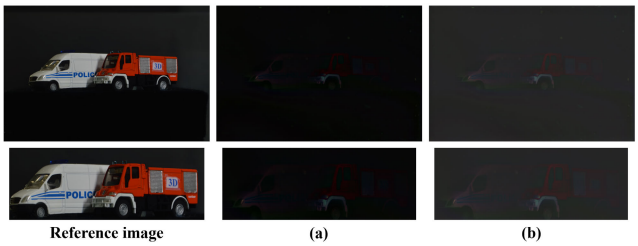

FIGURE 17. 3D reconstructed peplograms by (a) conventional peplography and (b) proposed wavelet peplography.

proposed method preserved the object photons and reduced the noise photons in the 3D scene as shown in Fig. 17 (b). The image contrast ratio can be enhanced as noise components are removed in the scene. Therefore, it is possible to recognize the word and visualize the shape of 3D objects more accurately compared to conventional peplography. Fig. 18 shows the image metric results to demonstrate the feasibility of our proposed method.

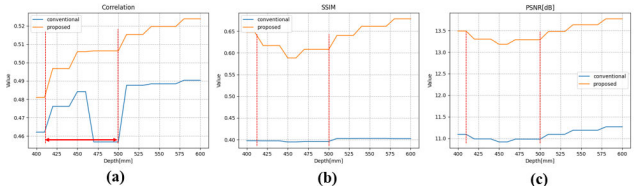

FIGURE 18. Image quality metrics via various reconstruction depths. (a) correlation, (b) structural similarity, and (c) peak signal-to-noise ratio.

Our proposed method has the best result through three image quality metrics. Especially, the PSNR and correlation values of our proposed method prove that our proposed method can visualize 3D object more accurately compared with conventional peplography. To compare the image quality metrics in detail, we arrange the value of the metrics in Table 2.

In conventional peplography, since the photon intensity may be decreased through the reconstruction process, it is more challenging to visualize 3D object under the dark situation. On the other hand, our proposed method can maintain the object photons without information loss and remove the noise photons only in the scene by using the adaptive coefficient threshold value. It can enhance the image contrast ratio and visualize 3D object under the dark scattering media condition more effectively. In addition, since the photon ratio is defined according to the light condition of the scene, our proposed method can visualize the 3D object in various light heavy scattering media conditions.

TABLE 2. Image metric differences in specific depths.

		430mm	450mm	470mm
Conventional	Correlation	0.4761	0.4841	0.4567
	SSIM	0.3971	0.3947	0.3958
	PSNR	10.9851	10.9162	10.9810
Proposed	Correlation	**0.4967**	**0.5059**	**0.5063**
	SSIM	**0.6168**	**0.5883**	**0.6080**
	PSNR	**13.2995**	**13.1797**	**13.2866**

V. CONCLUSION

In this paper, we have proposed a method that can enhance the visual quality of 3D image under heavy scattering media conditions. Conventional peplography utilizes photon counting technique to detect the object photons through the peplogram. Moreover, it can reconstruct 3D images to enhance the visual quality through the reconstruction process of integral imaging. However, it may not provide accurate 3D object information, because Poisson random process causes the photon intensity fluctuation and may detect the scattering media photons. In addition, it may not deal with various light scattering media conditions. In contrast, since our proposed method can reduce the scattering media photons and remain the object photons simultaneously by using multi-level decomposition, it can enhance the visual quality of 3D reconstructed peplogram. Moreover, it can adjust the photon ratio to visualize 3D object accurately even under the various light scattering media situations. We believe that our proposed method can be used for the autonomous vehicle camera system that requires accurate 3D object information under heavy scattering media situations with various light conditions. Moreover, if we can compose a sufficient pair image dataset with heavy scattering media and a clear situation, it can utilize machine learning such as a generative adversarial network to enhance the image visual quality. Therefore, we will use the machine learning technique by using wavelet peplography in the future.

ACKNOWLEDGMENT

(Myungjin Cho and Min-Chul Lee contributed equally to this work.)

REFERENCES

[1] Y. Wang, W.-L. Chao, D. Garg, B. Hariharan, M. Campbell, and K. Q. Weinberger, "Pseudo-LiDAR from visual depth estimation: Bridging the gap in 3D object detection for autonomous driving," in *Proc. IEEE/CVF Conf. Comput. Vis. Pattern Recognit. (CVPR)*, Jun. 2019, pp. 8445–8453.

[2] S. Zang, M. Ding, D. Smith, P. Tyler, T. Rakotoarivelo, and M. A. Kaafar, "The impact of adverse weather conditions on autonomous vehicles: How rain, snow, fog, and hail affect the performance of a self-driving car," *IEEE Veh. Technol. Mag.*, vol. 14, no. 2, pp. 103–111, Jun. 2019.

[3] Y. Schechner, S. Narasimhan, and S. Nayar, "Instant dehazing of images using polarization," in *Proc. IEEE Comput. Soc. Conf. Comput. Vis. Pattern Recognit. (CVPR)*, Dec. 2001, p. 1, doi: 10.1109/CVPR.2001.990493.

[4] K. He, J. Sun, and X. Tang, "Single image haze removal using dark channel prior," *IEEE Trans. Pattern Anal. Mach. Intell.*, vol. 33, no. 12, pp. 2341–2353, Dec. 2011, doi: 10.1109/TPAMI.2010.168.

[5] Q. Zhu, J. Mai, and L. Shao, "A fast single image haze removal algorithm using color attenuation prior," *IEEE Trans. Image Process.*, vol. 24, no. 11, pp. 3522–3533, Nov. 2015, doi: 10.1109/TIP.2015.2446191.
[6] Y. Li, R. T. Tan, and M. S. Brown, "Nighttime haze removal with glow and multiple light colors," in *Proc. IEEE Int. Conf. Comput. Vis. (ICCV)*, Dec. 2015, pp. 226–234.
[7] K. Soltanlou and H. Latifi, "Three-dimensional imaging through scattering media using a single pixel detector," *Appl. Opt.*, vol. 58, no. 28, pp. 7716–7726, 2019, doi: 10.1364/AO.58.007716.
[8] B. L. Cai, X. M. Xu, K. Jia, C. M. Qing, and D. C. Tao, "Dehazenet: An end-to-end system for single image haze removal," *IEEE Trans. Image Process*, vol. 25, no. 11, pp. 5187–5198, Aug. 2016, doi: 10.1109/TIP.2016.2598681.
[9] H. Zhang, V. Sindagi, and V. M. Patel, "Multi-scale single image dehazing using perceptual pyramid deep network," in *Proc. IEEE/CVF Conf. Comput. Vis. Pattern Recognit. Workshops (CVPRW)*, Jun. 2018, pp. 902–911.
[10] H. Dong, J. Pan, L. Xiang, Z. Hu, X. Zhang, F. Wang, and M.-H. Yang, "Multi-scale boosted dehazing network with dense feature fusion," in *Proc. IEEE/CVF Conf. Comput. Vis. Pattern Recognit. (CVPR)*, Jun. 2020, pp. 2157–2167.
[11] M. Cho and B. Javidi, "Peplography—A passive 3D photon counting imaging through scattering media," *Opt. Lett.*, vol. 41, no. 22, pp. 5401–5404, 2016, doi: 10.1364/OL.41.005401.
[12] G. A. Morton, "Photon counting," *Appl. Opt.*, vol. 7, pp. 1–10, Jan. 1968.
[13] M. D. Srinivas and E. B. Davies, "Photon counting probabilities in quantum optics," *Optica Acta, Int. J. Opt.*, vol. 28, no. 7, pp. 981–996, Jul. 1981.
[14] W. Goodman, *Statistical Optics*. Hoboken, NJ, USA: Wiley, 1985.
[15] E. A. Watson and G. M. Morris, "Comparison of infrared up conversion methods for photon-limited imaging," *J. Appl. Phys.*, vol. 67, no. 10, pp. 6075–6084, May 1990.
[16] G. Lippmann, "La photographie integrale," *Comp. Rendus Math. Academie des Sci.*, vol. 146, no. 9, pp. 446–451, 1908.
[17] J. S. Jang and B. Javidi, "Three-dimensional synthetic aperture integral imaging," *Opt. Lett.*, vol. 27, no. 13, pp. 1144–1146, 2002, doi: 10.1364/OL.27.001144.
[18] S.-H. Hong, J.-S. Jang, and B. Javidi, "Three-dimensional volumetric object reconstruction using computational integral imaging," *Opt. Exp.*, vol. 12, no. 3, pp. 483–491, 2004, doi: 10.1364/OPEX.12.000483.
[19] B. Cho, P. Kopycki, M. Martinez-Corral, and M. Cho, "Computational volumetric reconstruction of integral imaging with improved depth resolution considering continuously non-uniform shifting pixels," *Opt. Lasers Eng.*, vol. 111, pp. 114–121, Dec. 2018, doi: 10.1016/j.optlaseng.2018.07.016.
[20] H. Yun, A. Llavador, G. Saavedra, and M. Cho, "Three-dimensional imaging system with both improved lateral resolution and depth of field considering non-uniform system parameters," *Appl. Opt.*, vol. 57, no. 31, pp. 9423–9431, 2018, doi: 10.1364/AO.57.009423.
[21] B. Tavakoli, B. Javidi, and E. Watson, "Three dimensional visualization by photon counting computational integral imaging," *Opt. Exp.*, vol. 16, no. 7, pp. 4426–4436, 2008, doi: 10.1364/OE.16.004426.
[22] I. Moon and B. Javidi, "Three-dimensional recognition of photon-starved events using computational integral imaging and statistical sampling," *Opt. Lett.*, vol. 34, no. 6, pp. 731–733, 2009, doi: 10.1364/OL.34.000731.
[23] D. Aloni, A. Stern, and B. Javidi, "Three-dimensional photon counting integral imaging reconstruction using penalized maximum likelihood expectation maximization," *Opt. Exp.*, vol. 19, no. 20, pp. 19681–19687, 2011, doi: 10.1364/OE.19.019681.
[24] J. Jung, M. Cho, and B. Javidi, "Three-dimensional photon counting integral imaging using Bayesian estimation," *Opt. Lett.*, vol. 35, no. 11, pp. 1825–1827, 2010, doi: 10.1364/OL.35.001825.
[25] M. Cho and B. Javidi, "Three-dimensional photon counting integral imaging using moving array lens technique," *Opt. Lett.*, vol. 37, no. 9, pp. 1487–1489, 2012, doi: 10.1364/OL.37.001487.
[26] M. Cho, "Three-dimensional color photon counting microscopy using Bayesian estimation with adaptive priori information," *Chin. Opt. Lett.*, vol. 13, no. 7, 2015, Art. no. 070301.
[27] J. Lee, M.-C. Lee, and M. Cho, "Three-dimensional photon counting imaging with enhanced visual quality," *J. Inf. Commun. Converg. Eng.*, vol. 19, no. 3, pp. 180–187, 2021, doi: 10.6109/jicce.2021.19.3.180.
[28] J. Lee, M. Cho, and M.-C. Lee, "Three-dimensional photon counting optical encryption with enhanced visual quality and security level," *IEEE Access*, vol. 9, pp. 128862–128869, 2021, doi: 10.1109/ACCESS.2021.3113670.
[29] M. Holschneider, R. Kronland-Martinet, J. Morlet, and P. H. Tchamitchian, "A real-time algorithm for signal analysis with the help of the wavelet transform," in *Wavelets*. Springer, 1990, pp. 286–297, doi: 10.1007/978-3-642-75988-8_28.
[30] I. Daubechies, "The wavelet transform, time-frequency localization and signal analysis," *IEEE Trans. Inf. Theory*, vol. 36, no. 5, pp. 961–1005, Sep. 1990, doi: 10.1109/18.57199.
[31] J. B. Weaver, Y. Xu, D. M. Healy, and L. D. Cromwell, "Filtering noise from images with wavelet transforms," *Magn. Reson. Med.*, vol. 21, no. 2, pp. 288–295, Oct. 1991, doi: 10.1002/mrm.1910210213.
[32] H. Choi and J. Jeong, "Despeckling images using a preprocessing filter and discrete wavelet transform-based noise reduction techniques," *IEEE Sensors J.*, vol. 18, no. 8, pp. 3131–3139, Apr. 2018, doi: 10.1109/JSEN.2018.2794550.
[33] M. Hupfel, A. Y. Kobitski, W. Zhang, and G. U. Nienhaus, "Wavelet-based background and noise subtraction for fluorescence microscopy images," *Biomed. Opt. Exp.*, vol. 12, no. 2, pp. 969–980, 2021, doi: 10.1364/BOE.413181.
[34] J. Lee, M. Kurosaki, M. Cho, and M.-C. Lee, "Noise reduction for photon counting imaging using discrete wavelet transform," *J. Inf. Commun. Converg. Eng.*, vol. 19, no. 4, pp. 276–283, 2021, doi: 10.6109/jicce.2021.19.4.276.
[35] B. Li, W. Ren, D. Fu, D. Tao, D. Feng, W. Zeng, and Z. Wang, "Reside: A benchmark for single image dehazing," *IEEE Trans. Image Process.*, vol. 28, no. 1, pp. 492–505, Aug. 2018.

JAEHOON LEE received the B.S. degree from Hankyong National University, Anseong, South Korea, in 2018, and the M.S. degree from the Kyushu Institute of Technology, Fukuoka, Japan, in 2020, where he is currently pursuing the doctoral degree. His research interests include integral imaging, three-dimensional (3D) computational reconstruction, night vision, photon counting, digital holographic microscopy, information security, and three-dimensional (3D) visualization.

MYUNGJIN CHO received the B.S. and M.S. degrees in telecommunication engineering from Pukyong National University, Pusan, South Korea, in 2003 and 2005, respectively, and the M.S. and Ph.D. degrees in electrical and computer engineering from the University of Connecticut, Storrs, CT, USA, in 2010 and 2011, respectively. He was a Researcher at Samsung Electronics, South Korea, from 2005 to 2007. Currently, he is a Full Professor with Hankyong National University, South Korea. His research interests include 3D display, 3D signal processing, 3D biomedical imaging, 3D photon counting imaging, 3D information security, 3D object tracking, 3D underwater imaging, and 3D visualization of objects under inclement weather conditions.

MIN-CHUL LEE received the B.S. degree in telecommunication engineering from Pukyong National University, Busan, South Korea, in 1996, and the M.S. and Ph.D. degrees from the Kyushu Institute of Technology, Fukuoka, Japan, in 2000 and 2003, respectively. He is an Associate Professor with the Kyushu Institute of Technology. His research interests include medical imaging, blood flow analysis, 3D display, 3D integral imaging, and 3D biomedical imaging.